

EFFECTS OF THE SCISSORS CONFIGURATION ON ROTOR AERODYNAMIC CHARACTERISTICS

Guo-Hua Xu Shi-Cun Wang Jing-Gen Zhao

Institute of Helicopter Technology, Nanjing University of Aeronautics and Astronautics
Nanjing 210016, P. R. China

Abstract

An experimental and analytical investigation on the aerodynamic characteristics of a helicopter scissors rotor has been made. The experiments are carried out on a model rotor rig and the variations of the rotor thrust and torque with scissors angles are investigated. The effects of two different configurations, i.e., Configuration L in which the lower blade is in front of the upper blade and Configuration U in which the upper blade is in front of the lower blade, on rotor performance are compared. The experimental results have shown that the thrust for Configuration L is greater than that for Configuration U, and the strong blade-vortex interaction may occur at some scissors angles. A free-wake analytical model is then developed for predicting the aerodynamic characteristics of a scissors rotor and validated by numerical examples. By using the model, the blade induced velocity, lift distribution and tip vortex displacement of the scissors rotor are calculated. Based upon the calculations, the variations of the thrust with scissors angles in the experiments are analyzed and the strong blade-vortex interaction occurring in the experiments is explained. Finally, several conclusions are presented.

1. Introduction

The scissors rotor configuration has been employed on the modern armed helicopters such as AH-64 Apache (Ref. 1) and Mi-28 Havoc as a tail rotor. A well-known advantage with such a scissors configuration is its improvement in rotor noise characteristics. Whether or not the configuration

can improve rotor performance is controversial. The Bell Helicopters' early experimental results on a scissors rotor (Ref. 2, 1974) showed that neither the variation of the scissors angle nor the variation of the vertical spacing between its pair produced change in hover efficiency. However, the Mil Design Bureau gave an opposite conclusion in 1996 (Ref. 3). The latter experiments on a whirl-tower have found important advantages in the scissors configuration, especially the increase in rotor thrust.

Refs. 2 and 3 might be two of the minority studies on helicopter scissors (tail) rotor aerodynamics in existing publications. Even in the two papers, no theoretical research was involved, nor was the research on detailed aerodynamic characteristics such as blade induced velocity and loading distribution given.

In order to make clear about the effects of the scissors rotor configuration, a model scissors rotor has been experimentally investigated on a 2-meter rotor rig in the present work. The thrust and torque of the rotor at different scissors angles are compared and the effects of Configuration L and Configuration U are discussed. The present experiments not only validate the experimental conclusion by Mil Design Bureau in Ref. 3, but also obtain the new conclusion that the strong blade-vortex interaction may occur at some scissors angles.

In order to understand the physics of the aerodynamic characteristics of a scissors rotor system, an analytical model is presented based upon rotor free-wake analysis. The model rotors in Ref. 3 and in the present experiments are taken as numerical examples, respectively. The calculations

Presented at the 27th European Rotorcraft Forum, Moscow, Russia, September 11-14, 2001

on the thrust of the scissors rotor further support the experimental conclusion in Ref. 3. By the calculations of the blade induced velocity and loading distribution, the experiment result that the thrust for Configuration L is greater than that for Configuration U, obtained in the present experiment, is analyzed. From the calculations of the rotor tip vortex displacement, the experimental result that the strong blade-vortex interaction may occur at some scissors angles is explained.

2. Experimental Investigation

2.1 Description of Experiments

The experiments are carried out on the 2-m rotor test rig at the Nanjing University of Aeronautics and Astronautics as shown in Figure 1. The model rotor consists of a pair of co-axial 2-bladed rotors, the upper and lower location of rotors are defined according to the positive thrust direction of the rotor shaft. In terms of the relative azimuths of upper and lower rotors, there are two different configurations. One is the configuration in which the lower blades are in front of the upper blades, called Configuration L (Ref. 3) and the other is the configuration in which the upper blades are in front of the lower blades, Configuration U.



Fig. 1 Scissors rotor on the 2-m rotor rig

The blades of the model rotor tested are rectangular and have no twist. The radius and chord of blades are 1.0m and 0.06m, respectively. The model rotor is 2.6m high above the ground and is operated at 1200 rpm.

The experiments in the present work are only

for hovering flight. As far as the tail rotor of a helicopter is concerned, hovering flight might be its more important working state. In forward flight, a tail rotor actually work at low blade pitch due to the unloading of the vertical fin, and thus the improvement in aerodynamics is less important when compared to hovering flight.

In the experiments, the scissors angle is changed for $\Delta\psi = 0^\circ, 30^\circ, 45^\circ, 60^\circ$ and 90° , and the vertical separation between a pair of rotors is chosen as $\Delta\bar{h} = h/R = 0.058$ and 0.10 . As a special case of the scissors rotor, the conventional rotor has $\Delta\bar{h} = 0$ and $\Delta\psi = 90^\circ$. The chosen blade pitch are $\phi_7 = 10^\circ$ and 16° , and the rotor thrust and torque are measured by using a 6-component balance and a torque one, respectively.

2.2 Experimental Results and Discussion

Figure 2 presents the variations of the rotor thrust with scissors angles for the pitch angle of 10° and the vertical separation of $0.1R$. The thrust of the corresponding conventional rotor, T_{conv} , is also shown in the figure for comparison purposes. The experimental results in Fig. 2 have indicated that the thrust of the scissors rotor is different for Configuration L and Configuration U. The thrust for Configuration L is greater than that for Configuration U and the maximum difference in the present experiments is about 5%. For both Configuration L and Configuration U, the rotor thrust varies with the scissors angles. As seen in the figure, the thrust reaches the maximum value at $\Delta\psi = 30^\circ$ for Configuration L. The present experiments obtain the similar results to those in Ref. 3, which thereby support the conclusion in Ref. 3 as mentioned previously. In Ref. 3's experiments, the wider blade (0.22m) and higher pitch (18°) were adopted and measurable thrust difference was

larger (over 10%) for the two different configurations (see Figure 6).

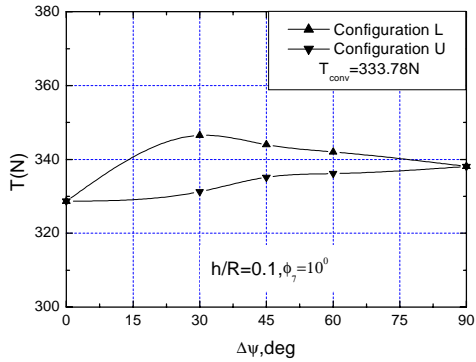


Fig. 2 Variations of the thrust with scissors angles in hover

The measurement results on torque are given in Fig. 3. As shown in the figure, the torque has little change with different scissors angles and configurations.

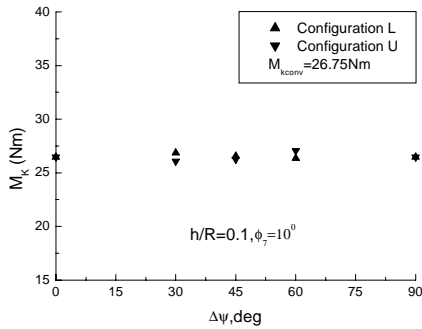


Fig. 3 Variations of the torque with scissors angles in hover

The present paper pays more attention to rotor thrust characteristics. For a tail rotor, different from a main rotor, the thrust gains may be more important than the torque (power) improvement in order to get better maneuvering characteristics in hover.

Figure 4 presents experimental results on the thrust and torque of the scissors rotor for the pitch angle of 16° . Note that the thrust and torque at $\Delta\psi = 45^\circ$ for Configuration L are not shown. In the experiments, a strange and intense phenomenon

rather like “rush flow” occurred at this scissors angle so that the measurement was interrupted. At

$\Delta\psi = 60^\circ$, the similar but somewhat weak

phenomenon was also encountered for Configuration L. The reason causing the phenomenon was not clear, but a conjecture on it was that the tip vortex from the upper rotor blade passed close to the lower rotor blade, which induced the local stall on the lower blade. This may be preliminarily judged from Fig. 4 where the torque increases and the thrust decreases for $\Delta\psi = 60^\circ$ and

Configuration L. It is worth notice that the similar “rush flow” phenomenon does not occur on other conditions of Configuration L and all conditions of Configuration U as seen in Fig. 4. In other words, the scissors configuration may result in strong blade-vortex interactions at some scissors angles.

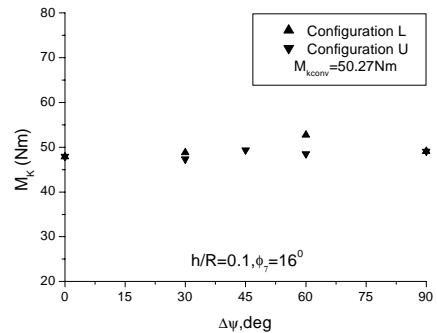
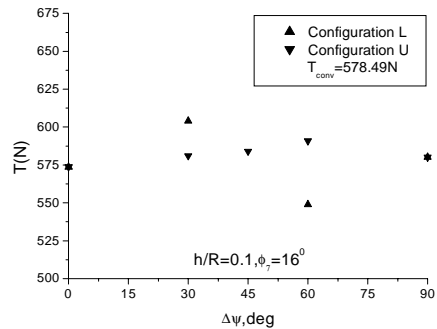


Fig. 4 Variations of the thrust and torque with scissors angles in hover ($\phi_7 = 16^\circ$)

When the vertical separation was $\bar{h}=0.058$, the experimental results (not shown) were similar to those for $\bar{h}=0.1$. However, again, the strong blade-vortex interaction was encountered at $\Delta\psi=60^\circ$ of Configuration L.

3. Theoretical Analysis

The azimuth spacing and vertical separation of a scissors rotor system substantially change the location and strength of wake vortices of upper and lower blades, and provides more blade-vortex encounter possibility. For such a vortical flowfield, the free wake method may be a proper analytical tool. The present paper modifies the authors' previous rotor free wake model (Refs 4 and 5) to develop a method for the aerodynamic analysis of a scissors rotor.

3.1 Solution of free wake

Here, the pseudo-implicit predictor-corrector (PIPC) method in Ref. 6 is used for free wake solution. The advantage with the PIPC is its better numerical characteristics and it has been adopted for the calculations of aerodynamic characteristics of swept-tip and coaxial rotors in Refs. 7 and 8.

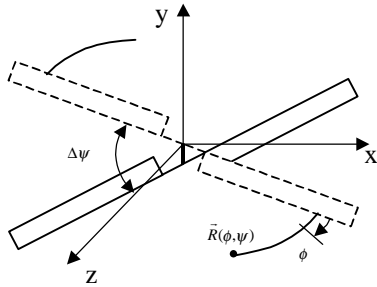


Fig. 5 Schematic of coordinate system

The rotor hub coordinate frame fixed to the upper rotor is chosen to define the wake geometry. As shown in Fig.5, the axes x and z are in rotation plane and the axis y is perpendicular to x and z , positive upward. A vortex filament shed from blades can be described geometrically as a space curve $\bar{R}(\phi, \psi)$ in the reference system, where ψ is

blade azimuthal angle and ϕ is a measure of the age of collocation points on a vortex filament. The governing equation describing the motion of a vortex filament can be expressed as

$$\frac{\partial \bar{R}(\phi, \psi)}{\partial \phi} + \frac{\partial \bar{R}(\phi, \psi)}{\partial \psi} = \frac{1}{\Omega} \bar{v}(\bar{R}(\phi, \psi)) \quad (1)$$

Where Ω is rotational speed, \bar{v} is the induced velocity on the points of vortex filaments and it includes the contributions from both upper and lower rotors.

In the present analysis, a five-point difference scheme with the equal difference steps, i.e., $\Delta\psi = \Delta\phi$, has been chosen for the solution, the difference equation of Eq. (1) can be written as

$$4\Omega(\bar{R}(\phi_j, \psi_k) - \bar{R}(\phi_{j-1}, \psi_{k-1})) = \Delta\psi \{ \bar{v}(\phi_j, \psi_k) + \bar{v}(\phi_{j-1}, \psi_k) + \bar{v}(\phi_j, \psi_{k-1}) + \bar{v}(\phi_{j-1}, \psi_{k-1}) \} \quad (2)$$

The initial condition of Eq. (2) is that vortex filaments leave blade trailing edges at initial instant, and the boundary condition is

$$\bar{R}(\phi, 2\pi + \psi) = \bar{R}(\phi, \psi) \quad (3)$$

Eq. (2) is an implicit equation, and the pseudo-implicit predictor-corrector scheme (Ref. 6) is used for its solution.

Predictor:

$$\begin{aligned} \bar{R}'(\phi_j, \psi_k) = & \bar{R}'(\phi_{j-1}, \psi_{k-1}) + \frac{\Delta\psi}{4\Omega} [\bar{v}^{n-1}(\phi_j, \psi_k) \\ & + \bar{v}^{n-1}(\phi_{j-1}, \psi_k) + \bar{v}^{n-1}(\phi_j, \psi_{k-1}) \\ & + \bar{v}^{n-1}(\phi_{j-1}, \psi_{k-1})] \end{aligned} \quad (4)$$

Corrector:

$$\begin{aligned} \bar{R}^n(\phi_j, \psi_k) = & \bar{R}^n(\phi_{j-1}, \psi_{k-1}) + \frac{\Delta\psi}{4\Omega} [\bar{v}'(\phi_j, \psi_k) \\ & + \bar{v}'(\phi_{j-1}, \psi_k) + \bar{v}'(\phi_j, \psi_{k-1}) + \bar{v}'(\phi_{j-1}, \psi_{k-1})] \end{aligned} \quad (5)$$

3.2 Blade aerodynamic model

Each blade is modeled using the second-order lifting line theory. The blade is divided into a finite

number of spanwise segments with the spanwise bound vortex located on the 1/4-chord line and the control point placed at the middle of the 3/4-chord line in each segment. The wake vortex filaments are trailed on blade trailing edges, and the bound circulation is solved by satisfying the boundary condition on the control points. The blade aerodynamic and wake model are coupled by the solution of the bound circulation.

Once the blade bound circulation is determined, the blade section lift per unit length can be easily calculated by applying the Joukowski law.

$$\frac{d\vec{L}_i}{dr} = \rho \vec{W}_i \times \vec{\Gamma}_i \quad (6)$$

The blade section drag is

$$dD_i = \frac{1}{2} \rho W_i^2 c c_{di} \quad (7)$$

The nondimensional blade section thrust can be written as

$$C_t \approx \frac{dL_i / dr}{0.5 \rho (\Omega R)^2 c} \quad (8)$$

Where ρ , W_i , Γ_i , c and c_{di} are air density, resultant section velocity, blade circulation, chord, and section drag coefficient, respectively.

After the blade section forces are known, rotor forces and moments can be determined.

3.3 Calculated Results and discussion

Some sample calculations on main rotors have previously been given in Refs 4, 5 and 7 by authors to validate the free wake method. Here, the comparisons of calculations and experiments are also made to show that the free wake method is suitable for the analysis of scissors rotors.

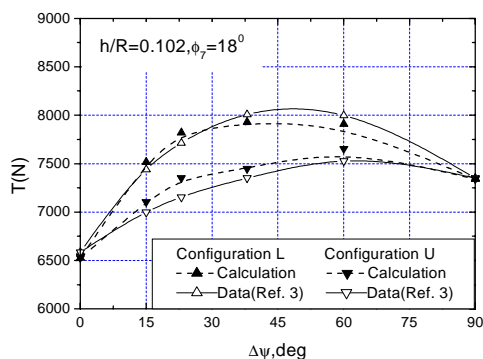


Fig. 6 Comparisons of calculated and experimental rotor thrust in hover

Figure 6 presents the comparisons of the thrust calculated by the present analysis and measured in Ref. 3. As seen in Fig. 6, the good correlation is achieved. Not only did the experimental results in Ref. 3 validate the present calculations, but also, more importantly, the present calculations further support the conclusion from experiments in Ref. 3. Figure 7 is the comparisons between the present experiments and calculations, again, the correlation is found to be good.

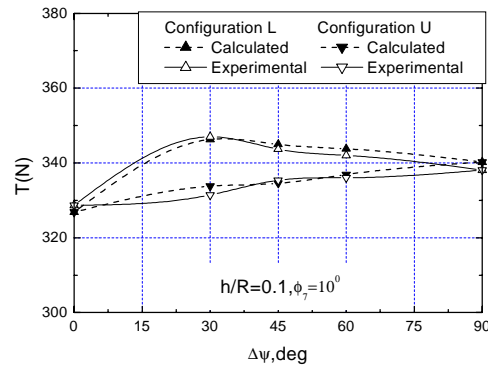


Fig. 7 Comparisons of calculated and experimental rotor thrust in hover

Therefore, a conclusion could be drawn from Figs 6 and 7, i.e., the thrust of scissors tail rotors indeed varies with different scissors angles and configurations, and the thrust for Configuration L is greater than that for Configuration U.

The present experimental model rotor in Fig. 1 will be further used to give numerical examples as follows.

Fig. 8 shows calculated induced velocity distributions along the blade span for Configuration L and Configuration U, in which the solid lines denote the induced velocity for the lower rotor and dashed lines denote that for the upper rotor. For both Configuration L and Configuration U, the induced velocities on the lower blade have larger changes near the tips than on the upper blade,

which is obviously because the vertical separation between the upper and lower rotors results in the close encounter of the upper-blade tip vortices with the lower blade. The interaction is somewhat similar to that of upper blade and lower blade for a coaxial twin-rotor system in Refs. 9 and 10.

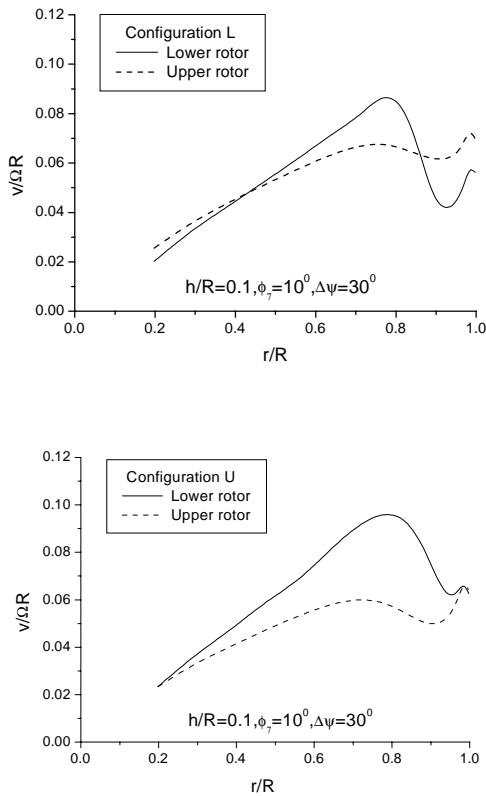


Fig. 8 Calculated induced velocity distribution for a scissors rotor

Fig. 9 shows the calculated non-dimensional blade section thrust distributions along a blade span in hover. As seen in the figure, for Configuration L, in comparison with the upper rotor, the lower rotor has greater thrust near the tips but smaller thrust for the inner part of the blade. In the case of Configuration U, the upper rotor has greater thrust along the whole span than the lower rotor. Although the thrust of the upper rotor for Configuration L is slightly smaller than that for Configuration U, the thrust of the lower rotor for Configuration L is larger than that for Configuration U, especially the thrust in the tip region of high dynamic pressure has more increase, therefore, the

total rotor thrust for Configuration L is still greater than the thrust for Configuration U (see Fig. 7).

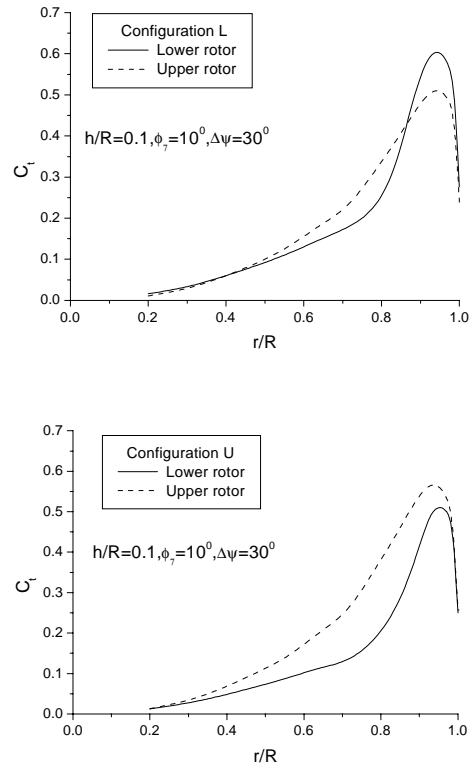


Fig. 9 Calculated spanwise blade section thrust distribution for a scissors rotor

Fig. 10 shows the calculated axial displacements of the tip vortex of the scissors tail rotor for four scissors angles of Configuration L. The marked point A denotes the encounter location of the preceding upper-rotor tip vortex with the following lower rotor. It should be noted that the upper rotor is located at $y/R=0.0$ and the lower rotor is located at $y/R=-0.1$. As shown in Fig. 10, the tip vortices from the upper rotor pass, at some distance, below the lower rotor when the scissors angle is 30° . In the case of $\Delta\psi = 45^\circ$, the upper-rotor tip vortices pass, in close proximity, above the lower rotor and the strong blade-vortex interaction may occur, which is explaining the experimental result in Fig. 4. With the further increase of scissors angles ($\Delta\psi = 60^\circ, 90^\circ$), the point A is moving away from

the lower blade. Therefore, a scissors rotor system probably results in stronger blade-vortex interaction than for a conventional rotor system, and usually the latter does not lead to a blade-vortex close encounter above the rotor plane in hover. In addition, as seen in the figure, since the lower rotor absorbs the wake of the upper rotor, the tip vortices of the upper rotor moves more quickly than those of the lower rotor.

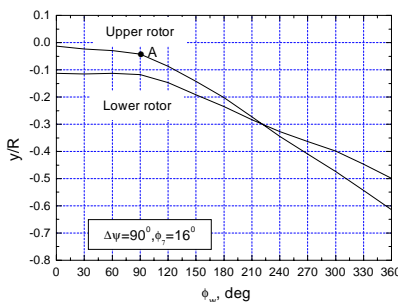
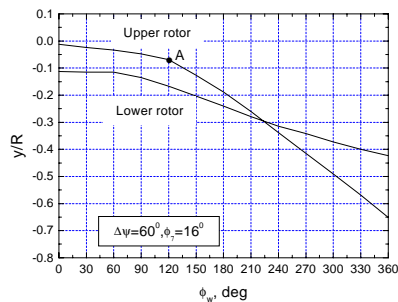
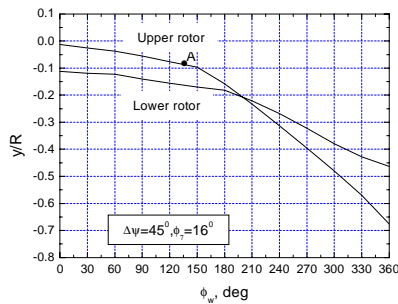
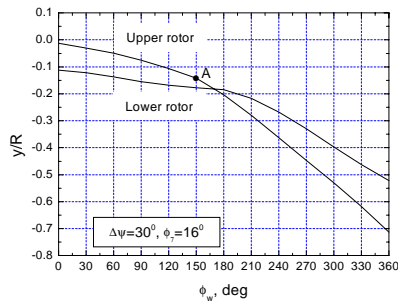


Fig. 10 Calculated axial displacements of tip vortices for a scissors rotor (Configuration L, $h/R=0.1$)

4. Conclusions

The experiments on a scissors rotor were conducted and the free-wake analytical method for the aerodynamic calculations of a scissors rotor was presented in this paper. The calculated and experimental results on rotor thrust were compared and the good correlation was reached. The blade induced velocity, the section thrust distribution and the tip vortex displacement for a scissors rotor were calculated and analyzed. From this investigation, the following conclusions have been drawn on a scissors (tail) rotor in hover:

a) A scissors rotor has more serious blade-vortex interaction problem than a conventional rotor, and the strong blade-vortex interaction may occur at some scissors configurations.

b) The thrust of a scissors rotor is different for Configuration L and Configuration U, and the difference depends upon rotor designs and blade pitch angles. The rotor thrust for Configuration L is greater than that for Configuration U.

c) The thrust of a scissors rotor varies with the scissors angles for both Configuration L and Configuration U. There is an optimum scissors angle for Configuration L, at which the rotor generates the maximum thrust.

d) The upper rotor of a scissors rotor system has stronger interaction to the lower one.

e) The tip vortex of the upper rotor moves more quickly than that of the lower one for a scissors rotor system.

References

1. Prouty, R. W. and Amer, K. B., The YAH-64 Empennage and Tail Rotor—A Technical History, Presented at the 38th Annual Forum of the American Helicopter Society, May 1982
2. Sonneborn, W. G. O. and Drees, J. M., The Scissors Rotor, Presented at the 30th Annual

Forum of the AHS, May 1974

3. Rozhdestvensky, M.G., Scissors Rotor Concept: New Results Obtained, Presented at the 52nd Annual Forum of the AHS, June 1996
4. Xu, G. H., Investigation on Aerodynamic Characteristics of Helicopter Rotor with New Blade Tip by Free Wake Analysis, Ph.D. Dissertation, Nanjing University of Aeronautics & Astronautics, 1996
5. Xu, G. H, Free Wake Calculation for Helicopter Rotor in Forward Flight, Journal of Nanjing University of Aeronautics & Astronautics, Vol. 29, No. 6, 1997
6. Bagai, A. and Leishman, J. G., Rotor Free-Wake Modeling using a Pseudo-Implicit Technique --- Including Comparisons with Experimental Data, Journal of the AHS, Vol.40, No.3, 1995
7. Xu, G. H. and Wang, S. C., An Analytical Method for Predicting Aerodynamic Characteristics of the Rotor with a Swept Tip, Acta Aerodynamica Sinica, Vol.17, No.3. 1999
8. Wang, P., Investigation on Aerodynamic Characteristics of Co-axial Rotors in Hover, M.S. Thesis, Nanjing University of Aeronautics & Astronautics, 1997
9. Saito, S. and Azuma, A., A Numerical Approach to Coaxial Rotor Aerodynamics, Presented at the 17th European Rotorcraft Forum, Sept. 1981
10. Andrew, M. J., Coaxial Rotor Aerodynamics in Hover, Vertica, Vol. 5, No. 2, 1983
11. Johnson, W., Helicopter Theory, Princeton University Press, 1980